21GRD02 BIOSPHERE

D4: Report on low energy electron scattering cross sections for molecules relevant in stratospheric chemistry and ozone depletion, including a user guide for the database of cross section collisions

Organisation name of the lead participant for the deliverable: **MPG**

Due date of the deliverable: **September 2025** (M36)

Actual submission date of the deliverable: 30 September 2025

Confidentiality Status: PU - Public, fully open

Deliverable Cover Sheet

Funded by the European Union. Views and opinions expressed are however those of the author(s) only and do not necessarily reflect those of the European Union or EURAMET. Neither the European Union nor the granting authority can be held responsible for them.

The project has received funding from the European Partnership on Metrology, co-financed from the European Union's Horizon Europe Research and Innovation Programme and by the Participating States.

Glossary

CS	Cross section
CR	Cosmic Radiation
eV	Electron volts
TDEACS	Total dissociative electron attachment cross sections
PDEACS	Partial dissociative electron attachment cross sections
MDICS	Metastable double ionization cross sections
PICS	Partial ionization cross section
TICS	Total ionization cross section
RIMS	Recoil ion momentum spectrometer
MCP	Microchannel plate
DLD	Delay-line anode

Contents

1 Summary

This report contains a user guide which is dedicated to elucidate the data provided in the zenodo repository [https://doi.org/10.5281/zenodo.15398189]. In this database cross sections are provided for electron impact ionization and dissociation of a number of atomic and molecular gases. The species contain the main constituents and trace gases in the Earth's stratosphere. The motivation is to collect and provide absolute cross sections to enable the simulation of the interaction of secondary electrons produced by primary extraterrestrial radiation. Such simulations require accurate data for an energy range from low threshold energies up to several hundred electron volts (eV) of energy. The data provided can be used to do more detailed and potentially more accurate calculations than presently available.

Furthermore, the collection of data on atmospheric relevant electron scattering prcesses within the BIOSPHERE project is summarized. This concerns data collected from literature and new measurements and calculations of the consortium.

.

2 Introduction

The influence of extraterrestrial particles like cosmic radiation (CR) on the chemistry and ozone density in the Earth's stratosphere are not well understood and normally neglected in atmospheric chemistry models. Cosmic radiation (CR) which can have higher energies but has lower flux. Most primary and secondary particles are stopped in the ionosphere, which concerns essentially all solar particles. Only particle showers initiated by the more energetic CR (> 1 GeV) can reach lower atmospheric layers like the stratosphere. Here ionization rates are up to 100 per second and per cm^3 and the ion density is around a few thousand per cm^3. There are observations that CR influences atmospheric properties such as cloud formation and ozone in the stratosphere [1]. In particular Liu demonstrated that stratospheric ozone concentration varies with the 11-year periodicity of the CR flux [2]. The significance of these observations and the mechanisms are under debate. Liu suggested a reaction model where anthropogenic chlorofluorocarbons (CFC) reaching the stratosphere are efficiently dissociated in reactions with secondary electrons from CR [3].

On the modelling side there are simulations of the atmospheric ionization density as, e.g., the AtRIS code [4] which is a GEANT4 based simulation of CR induced atmospheric particle showers providing ionization densities as function of the incoming radiation energy and the altitude. In principle this data can be the basis for modelling the atmospheric ion chemistry and the influence of CR showers on the relevant quantities like the ozone column density. On the other hand existing simulations of the ionization densities use the so-called W-value to convert the kinetic energies of the secondary electrons in the particle showers into the resulting number of electron-ion pairs. The W-value is a mean energy value required to produce an electron-ion pair which for atmospheric processes is normally determined for the nitrogen molecule. Here no specific molecular reactions are considered and, therefore, this approach strongly simplifies modeling but it cannot accurately reproduce the collisional products of the numerous atmospheric constituents.

Here we quantify the molecular processes involving low-energy electrons that affect the atmospheric dynamics. Fundamental data on the interaction of low-energy electrons with atmospheric gases of both natural and anthropogenic origin is provided. These include cross sections for ionization, dissociative electron attachment and fragment-ion production

of atmospheric constituents and trace gases. The data are collected from literature and also include data measured within the BIOSPHERE project/Work Package 3 [5]. The data provided can be used to do more detailed and more accurate calculations [6].

3 User guide for electron interaction cross sections collected in the repository

The data repository includes cross sections for the reactions (I) ionization and (II) electron attachment. One data file contains data for a particular reaction and a specific molecule.

Electron scattering data for the following species are included: N_2, O_2, O_3, H_2O, CO_2, Ar, Ne, H_2, He, Xe, N_2O, NO_2, NO, CH_4, CHF_3, $CHClF_2$, CCl_2F_2, $CClF_3$, CF_4, CH_2Cl_2.

The species considered include the standard main constituents of the Earth atmosphere. Furthermore, trace gases are included which are relevant for ozone-chemistry and ozone depletion.

Data are provided for electron impact ionization (providing positive ions) and dissociation. Furthermore, total cross sections for dissociative electron attachment (providing negative fragment ions) for a number of chlorofluorocarbons and chlorofluoromethanes are included.

3.1 Ionization

Ionization describes reactions of electrons with kinetic energy E_0 with a molecule ABC of the following form

$$\begin{aligned} e^-(E_0) + ABC &\rightarrow 2e^- + ABC^+ && \text{(ionization)} \\ &\rightarrow 2e^- + AB^+ + C && \text{(dissociative ionization)} \\ &\rightarrow 2e^- + A^+ + B + C \\ &: \end{aligned}$$

Each individual reaction is described by the partial ionization cross section (PICS). The sum of all reactions is described by the total ionization cross section (TICS).

For each species a file in ASCII format is provided. As an example, in Fig. 1 the top part of the file with total single and double ionization cross sections for CF_4 is shown. The file name includes the general reaction and the species (e.g. “ionization CF_4”). The first 8 lines of the file contain the following information:

Line 1: general reaction considered (e.g. ionization)

Line 3: species (e.g. CF_4)

Line 4: type of cross section “total ionization”

Line 5: reference where the data is found

Line 6: information on accuracy of the data

Line 8 and higher: table with cross sections

After the first table with total cross sections, tables for partial ionization cross section data are given in the same format.

```
Ionization

(CF4)
Total Single Ionization Cross Section
Dogan, M., Wolff, W., Mootheril, D. M., Pfeifer, T., & Dorn, A. Electron impact single and double ionization and dissociation
The overall uncertainty of the absolute cross sections obtained is estimated to be ~ ±10 %.

Electron energy [eV] σ[10e-16 cm^2]

30      1.353
40      2.217
70      3.893
100     4.136
200     3.759
400     2.824
600     2.311
800     1.922
1000    1.688

(CF4)
Total Double Ionization Cross Section
Dogan, M., Wolff, W., Mootheril, D. M., Pfeifer, T., & Dorn, A. Electron impact single and double ionization and dissociation
The overall uncertainty of the absolute cross sections obtained is estimated to be ~ ±10 %.

Electron energy [eV] σ[10e-16 cm^2]

70      0.03233
100     0.09464
200     0.1352
400     0.09188
600     0.05478
800     0.05209
1000    0.03894
```

Figure 1. ASCII data file for the CF_4 cross sections showing the total single ionization cross section (top part) and the total double ionization cross section. For details see text.

3.2 Electron attachment

Electron attachment describes reactions of electrons with kinetic energy E_0 with a molecule ABC of the following form

$$
\begin{aligned}
e^-(E_0) + ABC &\rightarrow ABC^- && \text{(attachment)} \\
&\rightarrow AB^- + C && \text{(dissociative attachment)} \\
&\rightarrow A^- + B + C \\
&: \\
\end{aligned}
$$

The first reaction is negligible for small molecular species since the autodetachment reaction, i.e. the reverse process, happens within a short time. On the other hand the dissociative electron attachment (DEA) can be faster than autodetachment and provide an ion and radicals. The processes occur at low energies E_0 typically below 10 eV and for many species there is DEA at energies below 1 eV. Therefore, DEA is potentially important for atmospheric particle showers, where abundant low energetic electrons are produced.

Each individual reaction is described by the partial DEA cross section (PDEACS). The sum of all reactions is described by the total DEA cross section (TDEACS).

For each species a file in ASCII format is provided. The file name includes the general reaction and the species (e.g. “total DEA CCl2F2”). The first 8 lines of the file contain the following information:

Line 1: general reaction considered (e.g. dissociative electron attachment (DEA))

Line 3: species (e.g. CCl2F2)

Line 4: type of cross section “total DEA cross section”

Line 5: reference where the data is found

Line 6: information on accuracy of the data

Line 8 and higher: table with cross sections

3.3 Final remarks

The data is being updated regularly. E.g. in the first version (Version 1.0.0, May 13, 2025) only data for ionization was included. The second version (Version 2, July 18, 2025) data for dissociative electron attachment of the various halocarbons was included. Presently these include TDEACS. The next version will include available PDEACS.

4 Report on collected cross sections and measurements of ionization cross sections

Important for ozone depletion are such substances which are stable in the troposphere and can make their way to the stratosphere (which is valid for the banned substances). There, chlorine and bromine release by interaction with UV radiation and low energy electrons will affect ozone chemistry. The mechanism of halogen release by interaction with low energy electrons is dissociative electron attachment (DEA) where the incoming electron is captured by the molecule forming a negative ion which dissociates, e.g., into Cl^- and a residual radical. Above 15 – 20 eV electron impact energy ionization (EI) and subsequent dissociation is possible.

4.1 Literature review on existing cross sections

PTB, MPG and NOVA have reviewed literature on the electron scattering cross sections on abundant atmospheric gases and CFC compounds. Following publications are the most relevant. The cross sections for atoms and diatomic molecules are collected in [12]. Relevant for the atmosphere are argon, N_2, CO, O_2 and NO. [14] reviews polyatomic molecules. Atmospheric relevance have CH_4, H_2O, HCl, NH_3, CO_2, N_2O, NO_2, O_3, OCS, SO_2, ClO_2. Furthermore [13] reviews important chlorofluorocarbons (CFCs). CF_4, CF_3Cl, CF_2Cl_2, $CFCl_3$, CCl_4. An important work on electron interactions with gases relevant for plasma processing is authored by Christophorou and Olthoff [15]. These gases include some carbonhalides and CFCs like CF_2Cl_2. A most recent compilation for the

nitrogenoxides N_2O, NO_2 and NO is given by [16]. There is much more literature on ionization and DEA of various species. Part of it is listed in table 1. In conclusion there is comprehensive and precise data for many molecules.

Target	DEA	EI	e-scattering	energy	experimetal	theory	Ref
Spalte2	Spalte3	Spalte4	Spalte5	Spalte6	Spalte7	Spalte8	Spalte9
CH2Cl2, ...	DEA			0 - 3.5 eV	X		J. Chem. Phys. 113, 1455 (2000)
CClF3, CClF2H, CCl2F2, CClFH2, CCl2FH, CCl3F	DEA			0 - 5 eV	X		Int. Journ. Mass Spectr. 205 (2001) 149-161
CF4 / C2F6			Total	100-1500	X		Radiation Physics and Chemistry 68 (2003) 79–83
CF3Cl	DEA		Vib	up to 3eV		X	J. Phys. B: At. Mol. Opt. Phys. 34 (2001) 3703–3716
CF3Cl / CH3Cl	DEA				X		J. Chem. Phys. 116, 5471 (2002)
CH2Cl2, CHCH3Cl2, and C(CH3)2Cl2	DEA					X	THE JOURNAL OF CHEMICAL PHYSICS 135, 134316 (2011)
CCl2F2	DEA			0 - 2 eV	X	X	J.Phys. Chem. A 2010, 114, 1474 - 1484
CCl3F / CCl2F2 / CClF3 / CHCl2F / CHClF2 / CHClF2 / CH2ClF		Total Ioniz		2 keV		X	Molecular Physics, 2014, Vol. 112, No. 13, 1816–1823
CH2Cl2			Elast	0 - 800 eV	X		J. Phys. B: At. Mol. Opt. Phys. 52 (2019) 025204 (12pp)
CC14, CFC13, CF2C12, and CF3Cl	DEA				X		Ber. Bunsenges. Phys. Chem. 86,252-261 (1982)
CF2Cl2, CF3Cl, CFCl3	DEA			0- 10 eV	X		Chem. Phys. 37 (1979) 21
CCl3F / CCl2F2 / CClF3 / CHCl2F / CHClF2 / CH2ClF		Total Ioniz		0 - 5000 eV		X	K.K. Irikura et al. / International Journal of Mass Spectrometry 222 (2003) 189–200
H2S, SiH4, CH4, CF4, CC14, SF6, C2H4, CC13F, CC1F3, and CC12F2			Total	10 - 1000 eV		X	PHYSICAL REVIEW A VOLUME 52, NUMBER 1 JULY 1995
CCl4, CCl3F, CCl2F2, CClF3, and CF4			Total	0.6 - 50 eV	X		J. Chem. Phys. 84, 813 (1986)
CH3Cl, CH2Cl2 , and CHCl3			Total	75 - 4000 eV	X		PHYSICAL REVIEW A VOLUME 59, NUMBER 2 FEBRUARY 1999
CH2Cl2			Elast	7 - 30 eV	X	X	PHYSICAL REVIEW A 97, 042702 (2018)
CF2Cl2 hydrated electrons	DEA				X		Phys. Chem. Chem. Phys. 2016, 18, 23910
CF2Cl2			Vib Elas Inelas	0.5 - 10 eV	X		A Mann and F Linder 1992 J. Phys. B: At. Mol. Opt. Phys. 25 1633
CF3Cl	DEA		Vib Elas Inelas	0.5 - 10 eV	X		A Mann and F Linder 1992 J. Phys. B: At. Mol. Opt. Phys. 25 1633
CClF3 and CCl3F		Diss Ioniz ir			X		Chemical Physics 330 (2006) 43–51
CCl4 , CCl3F, CCl2F2 , and CClF3		Abs Total			X		J. Chem. Phys. 121, 11653 (2004);
CHCl3	DEA				X		J. Chem. Phys. 107, 8955 (1997)
CHCl3, CCl4	DEA			0 - 1 eV	X		J. Chem. Phys. 107 (1997) 8955
CCl4, CCl3F, CCl2F2, CClF3, CF4, CHCl3, CH2Cl2, and CH3Cl					X		Int Journal of Mass Spectrometry and Ion Processes 125 (1993) 81-93
CH2Cl2			Electronic	1500 eV	X		Journal of Quantitative Spectroscopy & Radiative Transfer 287 (2022) 108227
CF3Cl	DEA				X		Eur. Phys. J. D (2012) 66: 51
			X			X	IEEE Transactions on Dielectrics and Electrical Insulation Vol. 16, No. 4; August 2009
CCl4 CHCl3, CH2Cl2 and CH3Cl	DEA			0 - 10 eV	X		Ber. Bunsenges. Phys. Chem. 84 580-585 (1980)
CF4, CCl4, CF2Cl2, CClF3 and CFCl3			Total	30 - 5000 eV		X	Nuclear Instruments and Methods in Physics Research B 254 (2007) 205–210
CClF3 and CCl3F		partial abso			X		International Journal of Mass Spectrometry 235 (2004) 223–228
CF3Cl	DEA		Vib			X	PHYSICAL REVIEW A 84, 052717 (2011)
CF3X and CF2X2(where X = H, Cl, Br,and I)			Total and elast	30 - 5000 eV		X	Journal of Electron Spectroscopy and Related Phenomena 210 (2016) 30–35
CF3Cl	DEA			0 - 10 eV	X		J. Phys. Chem. B 1998, 102, 824-830

Table 1. Collected most important publications for electron impact ionization and DEA of atmospheric relevant gases. Included are molecular species (first column), process (second and third columns), Type of cross section (fourth column), experimental or theoretical work (fifth and sixth column), reference (seventh column).

4.2 The measurement apparatus for MPG data

The MPG measurements are performed with a recoil ion momentum spectrometer (*RIMS*) [7]. A schematic drawing of the setup is shown in Fig. 2. The whole system is placed in a high-vacuum chamber at 10^{-8} mbar residual gas pressure. An electron gun produces a pulsed electron beam whose kinetic energy can be adjusted from a few eV up to 2 keV. The pulses have a repetition rate of 15.75 kHz and the pulse duration is 20 ns. The beam is guided by means of an axial magnetic field of 20 Gauss into an effusive gas beam exiting from metallic capillary with an inner diameter of 1.0 mm placed perpendicular to the electron beam. The effusive gas flow is controlled by a precision leak valve and the pressure in the chamber is kept around 1.5×10^{-7} mbar during operation of the gas beam. The target density in the effusive beam is around 10^{13} cm^{-3}. The ions produced in collisions are collected by a short
two-stage spectrometer with a total length of 11 cm and nine electrode rings of 9 cm inner diameter, each set at 10 mm apart, divided into three sections. The drift length is twice the acceleration length satisfying the Wiley–McLaren geometry [8] for the time-focusing condition. This is needed to prevent the spread of flight times of the ions with different starting positions due to the size of the interaction region of 2 mm along the spectrometer

axis. The first two electrodes, as shown in Fig. 2, define the pusher region, where the needle is positioned at half the distance between them. While the projectile pulse traverses the spectrometer, the interaction region is kept field-free to avoid any deflection of the electron beam. With a delay of 100 ns, voltage pulses of +100 *V* and +40 *V* are applied to the first pusher electrode and the needle, respectively. Thus, the ions are extracted from the interaction region and pushed into the acceleration section. This region is defined by the set of four electrodes, which are connected in series by 100 kΩ resistors, where electrode two is on ground and electrode five at -184 V. The voltage gradient of 224 V/35 mm accelerates and drives the ions into a field free region of 70 mm defined by the following electrodes and two subsequent grids kept at -184 V. A strong electric field is applied between the final grid and front of the *MCPs* set at -184 and -2600 V, respectively, accelerating the ions to higher energies for good detection efficiency before hitting the front *MCP*.

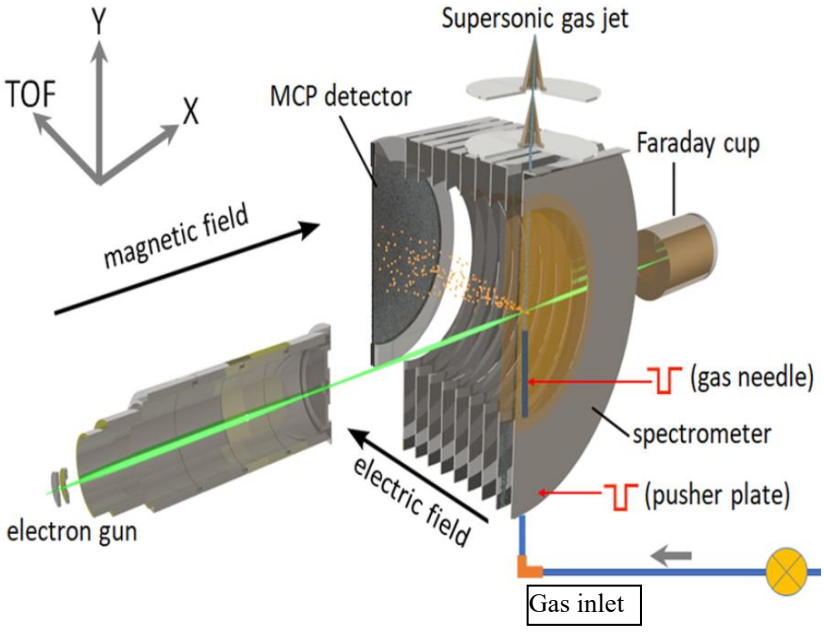

Figure 2. Illustration of the electron gun, the ion momentum spectrometer (sections allow views of electron and ion trajectories), and the gas mixing setup. The supersonic gas jet above the spectrometer was not in operation in this work.

All pulsed voltages are triggered by the electron pulses. Different voltage settings on the pusher and needle were probed with commitment to optimize the time-focusing condition as well as the detection of the full momentum distribution of the ions.
The time difference between the electron pulse signal and the detector *MCP* signal provides the time-of-flight information. The amplified electron cloud produced by the *MCPs* hits on a position-sensitive delay-line anode (*DLD* configuration), which records the X and Y-hit position distribution of the ions on the detector.19 The time and hit position signals are fed to a multi-hit time-to-digital converter, and the raw data events are recorded in list file mode by the *Cobold* data acquisition and analysis software.20 The X–Y coordinates of

the setup are defined as follows: the X-axis (horizontal) is along the electron beam and the Y-axis (vertical) is perpendicular to the electron beam and the extraction direction (Fig. 2).

4.3 Absolut normalization of the cross sections

The number of detected ions depends on many experimental parameters. In addition to the cross section, these are the electron beam current, the gas density, the size of the interaction volume between the electron beam and the gas target, the duration of the measurement and the detection efficiency. Most of these parameters are difficult to determine with sufficient accuracy. Therefore, many experiments in the past were conducted using the relative flow technique [9, 10]. Here the gas under investigation is mixed with a reference gas for which the cross section is known. Therefore, for both gases the geometrical interaction volume, the electron beam current and the measurement time are identical. Then, the cross section $\sigma_{T^+}(E)$ for the probe gas T at impact energy E is determined by the formula:

$$\sigma_{T^+}(E) = \sigma_{R^+}(E)\frac{\tilde{N}_{T^+}(E)}{\tilde{N}_{R^+}(E)} \tag{1}$$

Here $\sigma_{R^+}(E)$ is the cross section for the reference gas R. $\tilde{N}_{R^+}(E)$ and $\tilde{N}_{T^+}(E)$ are the corrected count numbers for the reference gas R and the test gas T, respectively. The measured count numbers for the reference and the test gases N_{R^+} and N_{T^+} must be corrected for two effects. One is the different detection efficiencies ε of the detector MCPs for the various ions which result essentially from different impact velocities on the detector. The detection efficiencies can be found from literature [11]. The second is a simple factor due to the mass dependence of the gas densities due to different molecular velocities.

$$\frac{\tilde{N}_{T^+}(E)}{\tilde{N}_{R^+}(E)} = \sqrt{\frac{m_R}{m_T}}\frac{\varepsilon_{R^+}}{\varepsilon_{T^+}}\frac{N_{T^+}(E)}{N_{R^+}(E)} \tag{2}$$

Here m_R and m_T are the molecular masses of the gases and ε_{R^+} and ε_{T^+} are the detection efficiencies for the reference gas ions and the test gas ions, respectively.

4.4 Exemplary data measured for CF_4 and CHF_3

In the following exemplary data for CF_4 and CHF_3 are presented, which are measured within the BIOSPHERE project.

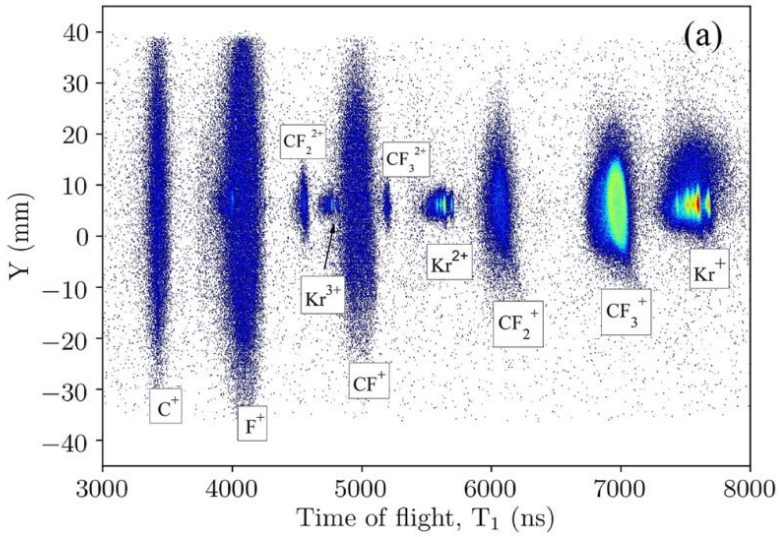

Figure 3. 2D-map of the Y-position on the detector and time-of-flight of a 200 eV electron collision with CF_4. The different islands shown correspond to different singly charged fragment ions which according to their masses vary in time-of-flight. The vertical spread of the islands is due to the initial velocities of the ions which results in a broad position distribution on the detector.

For measuring ionization cross sections for molecular gases it is important to detect all ions produced. This is a major challenge since due to their considerable kinetic energies which they obtain from the molecular dissociation the ions can easily escape the acceptance range of the spectrometer. Therefore, we apply relatively high extraction fields in combination with a short flight path and a large detector size (8 cm). In case of CF_4 gas the majority of the dissociating ions of CF_4 can have kinetic energies that can reach up to 15 eV which occurs, e.g. in dissociative double ionization channels. Figure 3 shows a two-dimensional map (2*D*-map) of the detected ion intensity as function of their y-position on the detector and time-of-flight for 200 eV electron impact energy. This diagram shows that essentially all ions with low to high momenta/kinetic energies are collected on the acceptance range of +/- 40 mm. There are no significant losses due to the kinetic energy of the ions. The ion time-of-flight spectrum is shown in Fig. 4. The TOF peaks of CF_3^+, CF_2^+, CF^+, F^+, CF_3^{2+}, CF_2^{2+} are clearly separated. Also seen are the krypton ions Kr^+, Kr^{2+}, and Kr^{3+}, are clearly discriminated in the gray filled pattern in Fig. 4. The time resolution of the setup allowed the separation of krypton isotopes, which occur as a mixture of six different, stable isotopes with masses of 78 (0.4%), 80 (2.3%), 82 (11.6%), 83 (11.5%), 84 (57.0%), and 86 (17.3%). The parent ion CF_4^+ is not expected to be found because its ionic states are not stable but dissociate within femtoseconds. The production of CF_3^+ dominates over other dissociation channels.

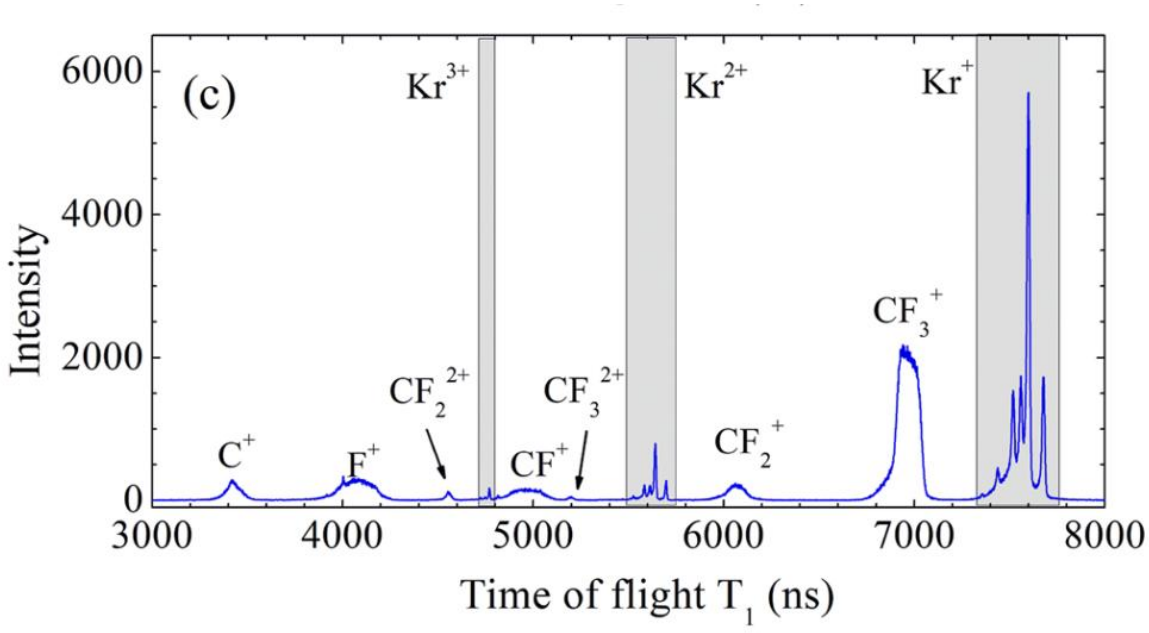

Figure 4. Time-of-flight spectrum for 200 eV electron impact ionization of CF_4 gas mixed with equal amount of krypton gas. The yields are shown on a linear scale. Ions from krypton are highlighted by gray regions.

From the integrated areas of the peaks the partial ionization cross sections are derived according to eqns. (1) and (2). The total ionization cross section is obtained from the sum of all partial ionization cross sections. One more correction is required since double ionization of the molecules can also yield the same singly charged fragment species and therefore falsify the cross sections. Therefore, in the present project coincidences between to singly charged ions originating from double ionization where measured. From these data the contribution of double ionization to the measured ion intensities was derived and used to correct the single ionization data.

For CF_4 the results are shown graphically in Fig. 5 and in tabular form in Table 2. The respective cross sections for CHF_3 are presented in Table 2. Here the mass resolution of the present setup is not sufficient to clearly identify hydrogen loss. Therefore, data are given as the sum of ionization cross section for processes with and without hydrogen loss.

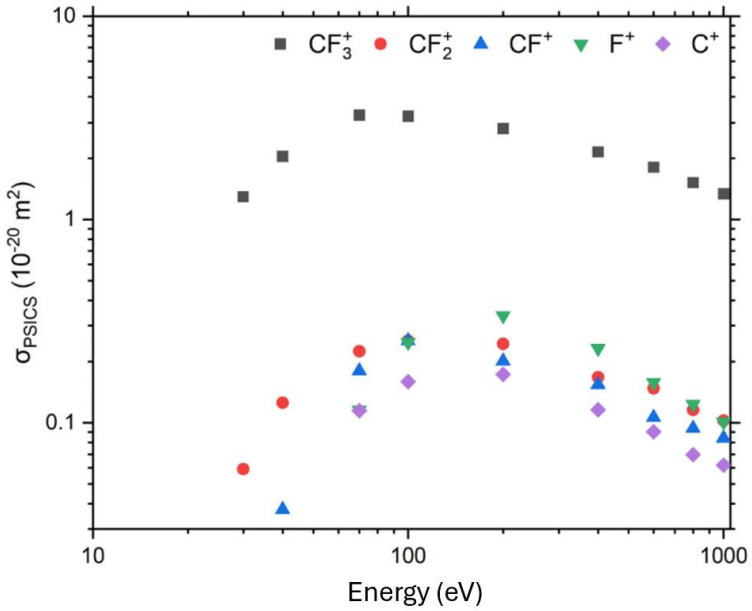

Figure 5. Absolute partial single ionization cross sections (PSICS) all observed fragments of CF_4.

E (eV)	CF_3^+	CF_2^+	CF^+	F^+	C^+	TSICS	CF_3^{2+}	CF_2^{2+}
30	1.294	0.059	—	—	—	1.353	—	—
40	2.047	0.126	0.037	—	0.007	2.217	—	—
70	3.257	0.225	0.181	0.115	0.115	3.893	0.005	0.013
100	3.219	0.254	0.254	0.249	0.160	4.136	0.010	0.026
200	2.804	0.245	0.202	0.336	0.173	3.759	0.014	0.036
400	2.153	0.168	0.155	0.233	0.116	2.824	0.009	0.023
600	1.808	0.148	0.106	0.158	0.090	2.311	0.006	0.017
800	1.519	0.116	0.094	0.123	0.070	1.922	0.004	0.012
1000	1.338	0.103	0.084	0.101	0.062	1.688	0.005	0.011

Table 2: TSICS, PSICS and MDICSs for CF_4 (in 10^{-20} m^2) as function of electron impact energy in eV

E (eV)	$C(H)F_3^+$	$C(H)F_2^+$	$C(H)F^+$	$(H)F^+$	$(H)C^+$	TSICS
20	0.177	0.201	—	—	—	0.378
30	0.401	0.798	0.207	—	—	1.405
40	0.544	1.220	0.407	—	0.036	2.206
70	0.654	1.713	0.693	0.090	0.150	3.300
100	0.664	1.852	0.794	0.134	0.196	3.639
200	0.551	1.660	0.731	0.132	0.177	3.251
400	0.422	1.162	0.472	0.122	0.112	2.290
600	0.348	0.977	0.388	0.095	0.084	1.891
800	0.287	0.851	0.335	0.075	0.071	1.620
1000	0.253	0.756	0.293	0.053	0.059	1.414

Table 3. TSICS and PSICS for CHF_3 (in 10^{-20} m^2) as function of electron impact energies in eV.

A more elaborate discussion of the measured cross sections in particular in comparison with existing published data is given in [24, 25].

4.5 Measurements on aerosols and smallest water droplets

Interactions of CR generated electrons and aerosols and water droplets might be of relevance for the stratospheric chemistry. BIRA-IASB provided data on sooth aerosols in the stratosphere. It turned out that respective targets are not available with sufficient density for the conduction of electron collision studies. On the other hand MPG succeeded in constructing a water cluster beam which consisted of aggregates of water molecules H_2O_n (n = 1-10). These clusters can be considered the smallest water droplets and electron collisions with these should be relevant for stratospheric processes. Figure 6 shows a time-of-flight spectrum taken by MPG which allows to identify the ionic reaction products. It shows that after ionization of a water molecule it abstracts a proton which is binding to the neighboring molecules while a OH radical is emitted. Therefore, for cluster ionization only protonated ions are observed. In addition neutral water molecules can be emitted depending on the energy transferred by the colliding electron. These findings were enabled by the simultaneous (coincident) detection of the scattered and the ionized electrons. The details of these studies on ionization of small water droplets are published in [19].

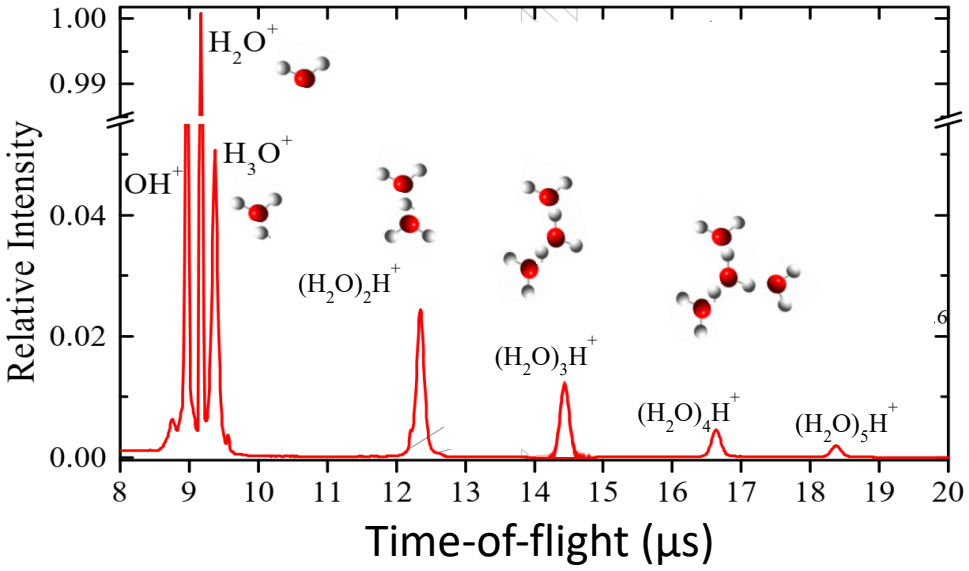

Figure 6. Time of flight spectrum for electron impact ionization of small water clusters. For each peak the according ion is indicated by its chemical formula and a graphical representation.

4.6 Angular differential cross sections measured by PTB

Measurements and calculations on electron scattering processes for various molecular species were carried out by PTB. The measurements where carried out with an electrostatic electron spectrometer which has high angular and energy resolution. Important in these studies was that PTB could demonstrate that theoretical models can reproduce the experimental data with sufficient good accuracy such that these calculations potentially can replace tedious measurements for molecules relevant for atmospheric modeling. First results were obtained for elastic electron scattering cross sections of ethanol [21]. In elastic scattering the projectile does not transfer energy but changes direction. More results were obtained for nitrous oxide for both processes, elastic scattering and ionization [23]. Here also angular differential cross sections were obtained which is relevant if particle tracks through a medium like the Earth atmosphere have to be simulated. As a highly relevant molecule for ozone depletion trichlorofluoromethane was studied by measuring elastic and inelastic electron scattering cross sections [17].

4.7 Electron scattering and O_2^- collisions measured by CSIC

CSIC has access to several unique measurement apparatuses. One is used to measure absolute total electron scattering cross sections with high accuracy. Within the BIOSPHERE project data for atmospheric relevant nitrogen oxides were taken. These are nitrogen dioxide N_2O and nitrous oxide N_2O for which electron scattering cross sections were measured over a large energy range from 1 up to 1000 eV [27, 28].

An important contribution was to perform measurements for peroxide anions (O_2^-) colliding with atmospheric gases. After free electron have lost their kinetic energy they are most likely captured by oxygen molecules. It is important to understand the subsequent reactions of O_2^-. CSIC have performed experiments for collisions of O_2^- with CO_2 molecules over a large energy range. At high impact energies beyond 500 eV they found so far unobserved reactions with the target molecule forming compound ions [20].

5 Acknowledgements

The project 21GRD02 BIOSPHERE has received funding from the European Partnership on Metrology, co-financed by the Horizon Europe Research and Innovation Program of the European Union and the participating States. Funder ID: 10.13039/100019599. Grant number: 21GRD02 BIOSPHERE.

6 References

[1] H. Svensmark and E. Friis-Christensen, J. Atmos. Terr. Phys. 59, 1225 (1997); H. Svensmark, Phys. Rev. Lett. 81, 5027 (1998); N. D. Marsh and H. Svensmark, ibid. 85, 5004 (2000).

[2] Q. B. Liu and L. Sanche, Phys. Rev. Lett. 87, 2001

[3] Qing-Bin Lu; *AIP Advances* **11,** 115307 (2021)

[4] Banjac, S., Herbst, K., & Heber, B. (2019), Journal of Geophysical Research: Space Physics, 124(1), 50.

[5] https://euramet-biosphere.eu/

[6] Dorn, A., Upendranath, P. (2025). https://doi.org/10.5281/zenodo.15398189

[7] M. Weyland, “Electronic excitation of atoms and dissociation of molecules by low energy electron collisions,” Ph.D. dissertation (Ruperto-Carola University of Heidelberg, Germany, 2016).

[8] W. C. Wiley and I. Mclaren, Rev. Sci. Instrum. 26, 1150 (1955).

[9] J. C. Nickel, P. W. Zetner, G. Shen, and S. Trajmar, J. Phys. E: Sci. Instrum. 22, 730 (1989).

[10] M. J. Brunger and S. J. Buckman, Phys. Rep. 357, 215 (2002)

[11] M. Krems, J. Zirbel, M. Thomason, and R. D. DuBois, Rev. Sci. Instrum. 76, 093305 (2005)

[12] Grzegorz P. Karwasz, Roberto S. Brusa and Antonio Zecca; RIVISTA DEL NUOVO CIMENTO Vol. 19, N. 3 (1996), One century of experiments on electron-atom and molecule scattering: a critical review of integral cross-sections. I. - Atoms and diatomic molecules.

[13] Grzegorz P. Karwasz, Roberto S. Brusa and Antonio Zecca; RIVISTA DEL NUOVO CIMENTO Vol. 24, N. 1 (2001), One century of experiments on electron-atom and molecule scattering: a critical review of integral cross-sections. II. – Polyatomic molecules.

[14] Grzegorz P. Karwasz, Roberto S. Brusa and Antonio Zecca; RIVISTA DEL NUOVO CIMENTO Vol. 24, N. 4 (2001), One century of experiments on electron-atom and molecule scattering: a critical review of integral cross-sections. III. - Hydrocarbons and halides.

[15] L. G. Christophorou and J. K. Olthoff, Springer Science + Business Media New York, 2004, Physics of Atoms and Molecules, Fundamental Electron Interactions with Plasma Processing Gases.

[16] Mi-Young Song, Jung-Sik Yoon, Hyuck Cho, Grzegorz P. Karwasz, Viatcheslav Kokoouline, Yoshiharu Nakamura, Jonathan Tennyson, Journal of Physical and Chemical Reference Data 48, 043104 (2019); Cross Sections for Electron Collisions with NO, N_2O, and NO_2.

[17] Dinger, M., Park, Y. and Baek, W. Y., Elastic and inelastic electron scattering cross sections of trichlorofluoromethane, Phys. Rev. A 111, 022809 (2025)

[18] Dinger, M., Park, Y., and Baek, W. Y., Differential elastic scattering and electron-impact ionization cross sections of nitrous oxide, Eur. Phys. J. D 78, 100 (2024)

[19] X. Ren, K. Hossen, S. Jia, J. Zhou, X. Xue, T. Pfeifer, A. Dorn, Electron-electron-ion triple-coincidence experiment of electron-initiated valence ionization of small water clusters, Phys. Rev. A 110, 042801 (2024)

[20] C. Guerra, M. Leiferman, A. I. Lozano, F. Aguilar-Galindo, S. Díaz-Tendero, J. C. Oller, P. Limão-Vieira, and G. García, Peroxide anion (O_2^-) collisions with CO_2 molecules in the energy range of 50–950 eV, J. Chem. Phys. 162, 054303 (2025)

[21] Combined experimental and theoretical study on the elastic electron scattering cross sections of ethanol. Dinger, M., Park, Y., Hepperle, P., Baek, W. Y., Eur. Phys. J. D 77, 52 (2023)

[22] Elastic and inelastic electron scattering cross sections of trichlorofluoromethane, Dinger, M., Park, Y. and Baek, W. Y., Phys. Rev. A 111, 022809 (2025)

[23] Dinger, M., Park, Y., and Baek, W. Y., Differential elastic scattering and electron-impact ionization cross sections of nitrous oxide, Eur. Phys. J. D 78, 100 (2024)

[24] W. Wolff. M. Dogan. H. Luna. L. H. Coutinho. D. Mootheril. Woonyong Baek. T. Pfeifer. A. Dorn, Absolute electron impact ionization cross-sections for CF_4, *Rev. Sci. Instrum.* 95, 095103 (2024)

[25] M. Dogan, W. Wolff, D. M. Mootheril, T. Pfeifer, A. Dorn, Electron impact single and double ionization and dissociation: revisiting CF_4 and CHF_3 with an improved experimental method, *PCCP* 27, 10057 (2025)

[26] X. Ren, K. Hossen, S. Jia, J. Zhou, X. Xue, T. Pfeifer, A. Dorn, Electron-electron-ion triple-coincidence experiment of electron-initiated valence ionization of small water clusters., Phys. Rev. A 110, 042801 (2024)

[27] A. I. Lozano, J. Rosado, F. Blanco, P. Limão-Vieira, and G. García, Integral Electron Scattering Cross Sections from N_2O for Impact Energies Ranging from 1 to 1000 eV, J. Phys. Chem. A 128, 699 (2024)

[28] A. I. Lozano, A. García-Abenza, J. Rosado, F. Blanco, J. C. Oller, P. Limão-Vieira and G. García, Electron scattering from NO_2: cross sections in the energy range of 1-1000 eV, Phys. Rev. A (under review)